

Study of the Crystallization Kinetics of $Zr_{60}Al_{15}Ni_{25}$ Bulk Glassy alloy by Differential Scanning Calorimetry

Zhijie Yan^{1,2,*}, Jinfu Li¹, Shunrong He¹, Honghua Wang¹ and Yaohe Zhou¹

¹State Key Laboratory of Metal Matrix Composites, School of Materials Science and Engineering, Shanghai Jiao Tong University, Shanghai, 200030, P.R. China

²Taiyuan Heavy Machinery Institute, Taiyuan, 030024, P.R. China

This paper investigates the crystallization kinetics of $Zr_{60}Al_{15}Ni_{25}$ bulk glassy alloy under isothermal annealing by differential scanning calorimetry (DSC). The results show that the incubation time is very small even at low annealing temperature (743 K) and increases slightly with the annealing temperature decreasing, which suggests a growth-controlled crystallization process. However, the exothermic peak width, reflecting the time for the actual crystallization process, increases greatly when annealing temperature decreases. The Avrami exponents indicate that the crystallization mechanism changes at different annealing temperatures. The change of the crystallization mechanism is attributed to the great difference of the mobility ability of atoms at different temperatures.

(Received November 11, 2002; Accepted February 27, 2003)

Keywords: crystallization kinetics, $Zr_{60}Al_{15}Ni_{25}$ bulk glassy alloy, differential scanning calorimetry

1. Introduction

A liquid alloy will be metastable with respect to crystallization when it cools below the liquidus temperature. If the liquid alloy is quenched sufficiently rapidly that the atoms freeze into a non-crystalline arrangement, an amorphous alloy is formed. Overcoming the tendency of conventional alloys to crystallize usually requires critical rates as high as 10^6 K/s, which can be attainable only by rapid quenching such as melt-spinning. The quenching methods to obtain high cooling rates result in sample thickness limited to less than $50\mu\text{m}$.¹⁾

Since 1988, a new class of multicomponent glassy alloys, as so-called bulk glassy alloys, has emerged. They can be synthesized at much lower cooling rates with dimensions reaching magnitude of mm.²⁻⁸⁾ The novel bulk glassy alloys exhibit a high resistance against crystallization in their supercooled liquid region, which provides an experimentally accessible time and temperature window to investigate, even isothermally, the crystallization behavior of the supercooled liquid.

$Zr_{60}Al_{15}Ni_{25}$ has been discovered as the first Zr-based bulk glass former with a wide supercooled liquid region ΔT_x (defined as the temperature region between glass transition temperature T_g and crystallization temperature T_x) as high as 77 K.⁴⁾ Li *et al.* has investigated the phase products during the crystallization of $Zr_{60}Al_{15}Ni_{25}$ glassy alloy by analytical transmission electron microscopy (ATEM) and X-ray diffraction (XRD).⁹⁾ However, little work has been done on the crystallization kinetics of this bulk glassy alloy. In this paper, crystallization kinetics of $Zr_{60}Al_{15}Ni_{25}$ bulk glassy alloy is investigated by differential scanning calorimetry (DSC).

2. Experimental

The ingot with nominal composition $Zr_{60}Al_{15}Ni_{25}$ was prepared by arc melting a mixture of pure Zr (99.9 mass%), Al (99.99 mass%) and Ni (99.9 mass%) metals in a water-cooled copper crucible under titanium-gettered argon atmosphere. To prevent segregation, the ingot was melted 4 times. A plate-like specimen with a cross-section of $1 \times 10\text{ mm}^2$ were produced by suction casting in a copper mold, and its glassy nature was verified by X-ray diffraction (XRD) using $\text{Cu-K}\alpha$ radiation. The crystallization process of the $Zr_{60}Al_{15}Ni_{25}$ bulk glassy alloy was characterized by non-isothermal and isothermal annealing in a differential scanning calorimeter (NETZCH, DSC 404) under flowing high purity argon. In the case of non-isothermal analysis, the DSC plot was recorded at a heating rate of 10 K/min. For the isothermal analysis, the glassy samples were firstly heated (at a rate of 50 K/min) to a fixed temperature (between 743 K and 758 K), and then held for a certain period of time until completion of crystallization. The Al_2O_3 and Al pans were utilized for the continuous heating and isothermal annealing respectively.

3. Results and Discussion

Figure 1 shows the XRD pattern of the as-cast $Zr_{60}Al_{15}Ni_{25}$ specimen, verified to be a single glassy phase. The non-isothermal DSC plot is shown in Fig. 2. The DSC trace shows an endothermic event, which is the characteristic of glass transition, followed by a single exothermic event corresponding to crystallization process. The glass transition temperature T_g and the onset temperature of crystallization T_x is 686 K and 758 K respectively. The supercooled liquid region ΔT_x is 72 K, which is slightly smaller than 77 K reported in literature.⁴⁾ The reason is that the heating rate is 10 K/min in our work but 40 K/min in literature⁴⁾ during the continuous heating.

The isothermal kinetics of crystallization of $Zr_{60}Al_{15}Ni_{25}$ bulk glassy alloy was investigated by DSC in supercooled

*Corresponding author: School of Materials Science and Engineering, Shanghai Jiao Tong University, Shanghai, 200030, P.R. China. E-mail: zjyan@sjtu.edu.cn (Z. J. Yan).

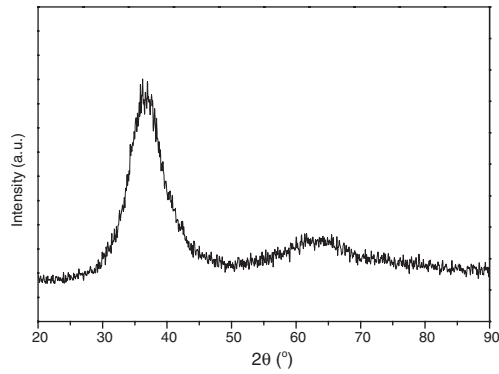


Fig. 1 The XRD pattern of the as-cast $\text{Zr}_{60}\text{Al}_{15}\text{Ni}_{25}$ specimen.

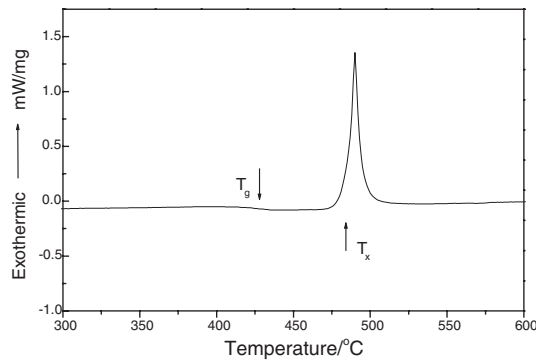


Fig. 2 The non-isothermal DSC trace of $\text{Zr}_{60}\text{Al}_{15}\text{Ni}_{25}$ bulk glass alloy.

liquid region (between 743 and 758 K). The DSC plots are shown in Fig. 3. All the DSC traces exhibit a single exothermic peak after a certain incubation period. The detailed DSC results are shown in Table 1. It can be seen that the incubation time τ (defined as the time scale between the time t_0 and $t_{1\%}$, t_0 is the time to reach the annealing temperature and $t_{1\%}$ the time to reach 1% crystallized volume fraction) is very short for different annealing temperatures. The change of τ is very small when the annealing temperature decreases, however, the exothermic peak width (referred to the time between 1% and 95% of transformation into the crystalline state) changes greatly, indicating a more

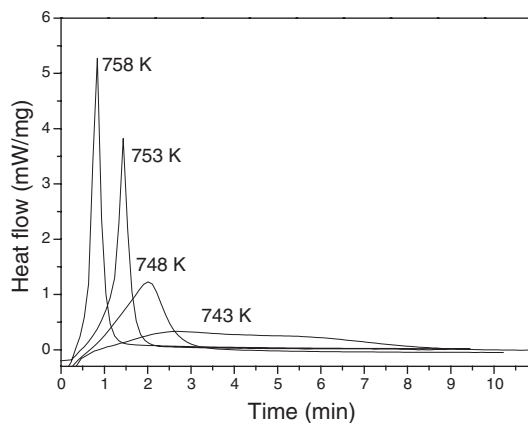


Fig. 3 The isothermal DSC plots of $\text{Zr}_{60}\text{Al}_{15}\text{Ni}_{25}$ bulk glass at different annealing temperatures.

Table 1 The kinetic parameters of $\text{Zr}_{60}\text{Al}_{15}\text{Ni}_{25}$ bulk glassy alloy at different annealing temperatures.

Annealing temperature (K)	743	748	753	758
Incubation time, τ (min)	0.52	0.41	0.39	0.31
Avrami exponent, n	1.51	2.32	3.8	4.15
Reaction constant, k (min^{-1})	0.24	0.60	0.93	1.79
$t_{95\%} - t_{1\%}$ (min)	7.73	2.75	1.42	0.82

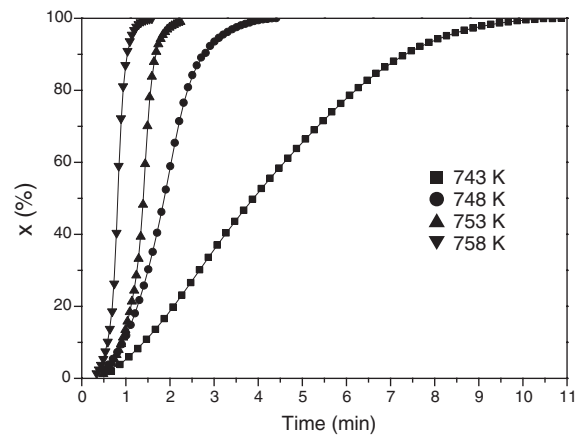


Fig. 4 The crystallized volume fraction as a function of annealing time of $\text{Zr}_{60}\text{Al}_{15}\text{Ni}_{25}$ bulk glass at different temperatures.

sluggish crystallization process.

It's assumed that the crystallized volume fraction x , up to any time t , is proportional to the partial area of the exothermic peak. Thus the volume fraction at a given time during the crystallization can be determined by measuring the partial area of the exothermic peak. The plots of the measurement results at different temperature are shown in Fig. 4. And their shapes are typical "s" type. The time evolution of the crystallized volume fraction can be modeled by the Johnson-Mehl-Avrami (JMA) equation as following:^{10,11)}

$$x(t) = 1 - \exp\{-[k(t - \tau)]^n\} \quad (1)$$

where $x(t)$ is crystallized volume fraction, t the annealing time, n a constant related to the dimensionality of nucleation and growth, and k a reaction rate constant which depends on temperature T and effective activation energy for crystallization E_c (which is the minimum energy needed to activate the crystallization) by

$$k = k_0 \exp(-E_c/RT) \quad (2)$$

in which K_0 is a constant and R the gas constant.

Based on eq. (1), an equation can be deduced as following:

$$\ln[-\ln(1 - x)] = n \ln k + n \ln(t - \tau) \quad (3)$$

Plotting $\ln[-\ln(1 - x)]$ vs. $\ln(t - \tau)$ at different annealing temperatures for the data $x = 15\% - 85\%$, the JMA plots can be obtained and shown in Fig. 5. The plots are nearly straight lines. The Avrami exponents n and the reaction rate constants k can be calculated from the slope and intercept of the lines and the detailed results are shown in Table 1. The Avrami exponents for different annealing temperatures vary from

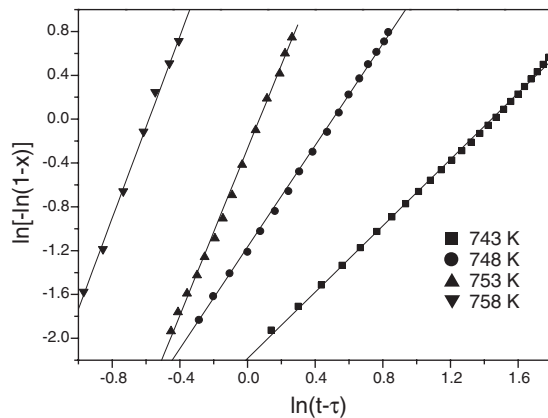


Fig. 5 The JMA plots for the crystallization of $\text{Zr}_{60}\text{Al}_{15}\text{Ni}_{25}$ bulk glass at different annealing temperatures.

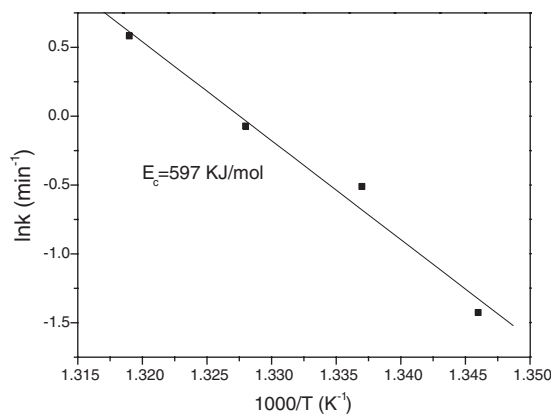


Fig. 6 The $\ln k$ vs. $1/T$ plot of $\text{Zr}_{60}\text{Al}_{15}\text{Ni}_{25}$ bulk glass, from which the effective activation energy is obtained.

1.51 to 4.15. Based on the plot $\ln k$ vs. $1/T$ shown in Fig. 6, the effective activation energy E_c is calculated to be 560 kJ/mol, which is much larger than $\text{Zr}_{55}\text{Cu}_{30}\text{Al}_{10}\text{Ni}_{12}$ ¹²⁾ and $\text{Zr}_{41}\text{Ti}_{14}\text{Cu}_{12.5}\text{Ni}_{10}\text{Be}_{22.5}$,¹³⁾ implying a higher thermal stability against crystallization.

The very small value of the incubation time and its slight change (the maximum change value is 0.21 min) for different temperatures suggest that the activation of crystallization starts from the growth of overcritical quenched-in nuclei. It has been found that the crystallization of $\text{Pd}_{43}\text{Ni}_{10}\text{Cu}_{27}\text{P}_{20}$ glassy alloy was influenced by the heterogeneous sites even after the sample was fluxed by B_2O_3 ,¹⁴⁾ indicating that the heterogeneous sites in the supercooled liquid of a glassy alloy are inevitable. The heterogeneous sites originate from the short-range orders in the glassy phase, as the so-called quenched-in nuclei, which provide the nucleation sites for the precipitation of the primary phase during the crystallization process.^{15,16)} And even, when the active size of the quenched-in nuclei is larger than the critical cluster radius at a given annealing temperature, these nuclei then simply grow with time. Under this condition, the alloy is spontaneously with the nuclei at a density corresponding to the density of the quenched-in nuclei. Hereby, it's assumed that there exist short-range orders in $\text{Zr}_{60}\text{Al}_{15}\text{Ni}_{25}$ bulk glassy alloy and the size of them is on the verge of and even larger

than the critical cluster radius at annealing temperatures between 743 and 758 K. As a result, during the crystallization, there needs little time to nucleate, verified by the very small incubation time and its slight change at different annealing temperatures.

The Avrami exponents varying from 1.51 to 4.15 suggest a diffusion-controlled three-dimensional growth during the crystallization of $\text{Zr}_{60}\text{Al}_{15}\text{Ni}_{25}$ bulk glassy alloy. At lower annealing temperatures (743 and 748 K), the smaller Avrami exponents (1.51 and 2.32) indicate the crystallization is governed by three-dimensional growth with a decreasing nucleation rate. The amorphous state of multi-component system with significant atomic size difference forms dense random packed atomic configuration.¹⁷⁾ Mobility of atoms in such atomic configuration is obviously difficult. The very large effective activation energy for crystallization E_c demonstrates that the atomic diffusion in Zr–Al–Ni system is very difficult, especially at low temperature. At the initial crystallization stage, there exist enormous number of short-range orders acting overcritical nuclei in the supercooled liquid, showing a spontaneously high nucleation rate. The growth of the overcritical cluster nuclei and formation of new nuclei need the atomic rearrangement. The difficult atomic diffusion at low temperature retards the nucleation and growth, resulting in a decreasing nucleation rate and very broad exothermic peak width (Fig. 3). At relatively high annealing temperatures (753 and 758 K), the larger Avrami exponents (3.8 and 4.15) imply a three-dimensional growth at an increasing nucleation rate. The atomic mobility at high temperature is relatively easy. The growth of the nuclei changes the composition in their neighborhood since the composition of the $\text{Zr}_{60}\text{Al}_{15}\text{Ni}_{25}$ alloy is close to eutectic point. The composition fluctuation results in an enhancement of the nucleation rate adjacent to the growing nuclei, which causes a chain reaction-like process, leading to a higher nucleation rate than in the initial supercooled liquid. So, the crystallization even completes within a very short time scale (0.82 min at 758 K).

4. Conclusion

In summary, the crystallization kinetics of $\text{Zr}_{60}\text{Al}_{15}\text{Ni}_{25}$ bulk glassy alloy was investigated under isothermal condition in a differential scanning calorimeter. The incubation time is very small even at low annealing temperature (743 K) and increases slightly with the annealing temperature decreasing, which suggests a growth-controlled crystallization process. However, the exothermic peak width, reflecting the time for the actual crystallization process, increases greatly with temperature decreasing, which is attributed to the difficulty of atomic diffusion verified by the much large effective active energy.

From the Avrami exponents, it can be known that the crystallization mechanism changes at different annealing temperatures. At lower annealing temperature (743 and 748 K), the crystallization process governed by three-dimensional growth at a decreasing nucleation rate, but by three-dimensional growth at an increasing nucleation rate at higher annealing temperatures (753 and 758 K). This is attributed to the facts that the crystallization process of $\text{Zr}_{60}\text{Al}_{15}\text{Ni}_{25}$ bulk

glassy alloy is growth controlled (at the initial crystallization stage, the alloy is spontaneously filled with overcritical nuclei at a density corresponding to the density of the quenched-in nuclei) and the atomic diffusion is difficult at lower temperatures but relatively easy at higher temperatures. The difficulty of atomic diffusion makes nucleation sluggish at lower temperatures, resulting a decreasing nucleation rate. However, at higher temperatures, the growth of the overcritical nuclei changes the composition in their neighborhood and results in an enhancement of the nucleation rate adjacent to the growing nuclei, which causes a chain reaction-like process, leading to a higher nucleation rate than in the initial supercooled liquid.

Acknowledgments

The work was financially supported by the National Natural Science Foundation of China (grant No. 50071032). The authors express their gratitude to Professor Jiang (Technical University of Denmark) for useful discussion.

REFERENCES

- 1) R. W. Cahn: in *Rapidly Solidified Alloys*, ed. H. H. Libermann, (Marcel Dekker, New York, 1993) p1.
- 2) A. Inoue, T. Zhang and T. Masumoto: *Mater. Trans., JIM* **30** (1989) 965–972.
- 3) A. Inoue, T. Zhang and T. Masumoto: *Mater. Trans., JIM* **31** (1990) 177–183.
- 4) A. Inoue, T. Nakamura, N. Nishiyama and T. Masumoto: *Mater. Trans., JIM* **33** (1992) 937–945.
- 5) A. Inoue, N. Nishiyama, K. Amiya, T. Zhang and T. Masumoto: *Mater. Lett.* **19** (1994) 131–135.
- 6) A. Inoue, Y. Shinohara and G. S. Gook: *Mater. Trans., JIM* **36** (1995) 1420–1426.
- 7) A. Inoue, N. Nishiyama and T. Matsuda: *Mater. Trans., JIM* **37** (1996) 181–184.
- 8) A. Inoue, W. Zhang, T. Zhang and K. Kurosaka: *Acta Mater.* **49** (2001) 2645–2652.
- 9) C. F. Li, J. Saida, M. Matsushida and A. Inoue: *Mater. Lett.* **44** (2000) 80–86.
- 10) M. A. Johnson and R. F. Mehl: *Trans. Am. Inst. Min., Metall. Pet. Eng.* **135** (1939) 416–442.
- 11) M. Avrami: *J. Chem. Phys.* **9** (1941) 177–190.
- 12) L. Liu, Z. J. Wu and J. Zhang: *J. Alloys Compd.* **339** (2002) 90–95.
- 13) Y. X. Zhuang, W. H. Wang, Y. Zhang, M. X. Pan and D. Q. Zhao: *Appl. Phys. Lett.* **75** (1999) 2392–2394.
- 14) J. Schroers, Y. Wu, R. Busch and W. L. Johnson: *Acta Mater.* **49** (2001) 2773–2781.
- 15) Y. Zhang, K. Hono, A. Inoue and T. Sakurai: *Acta Mater.* **44** (1996) 1497–1510.
- 16) C. Fan, D. V. Louzguine, C. Li and A. Inoue: *Appl. Phys. Lett.* **75** (1999) 340–342.
- 17) T. Zhang, A. Inoue and T. Masumoto: *Mater. Trans., JIM* **32** (1991) 1005–1010.